Journal of Optoelectronics and Biomedical Materials Vol. 7, Issue 4, October - December 2015 p. 85 - 91

MICROWAVE-ASSISTED SYNTHESIS AND ENHANCED PHOTOCATALYTIC ACTIVITY OF CARBON NANOTUBES SUPPORTED ZnS NANOPARTICLES

G. WAN[a, b], G. WANG[a, b *]
[a]*Key Laboratory of Ministry of Education for Application Technology of Chemical Materials in Hainan Superior Resources, The College of Materials and Chemical Engineering, Hainan University, Haikou 570228, P. R. China*
[b]*Key Laboratory of Chinese Education Ministry for Tropical Biological Resources, Hainan University, Haikou 570228, P. R. China*

Carbon nanotubes (CNTs) supported ZnS nanoparticles were prepared by a microwave-assisted chemical reaction between $Zn(Ac)_2·2H_2O$ and $Na_2S·9H_2O$ in glycol solution with CNTs, which were pretreated by oxidization in concentrated HNO_3. The CNTs supported ZnS were characterized using transmission electron microscopy and X-ray diffraction. ZnS crystallite densely decorated on CNTs with the diameter about 1.1 nm. The photoluminescence (PL) spectrum shows that the PL peaks of the CNTs supported ZnS have a small blue shift in comparison with the bulk of ZnS. Studies on methylene blue degradation revealed that CNTs could effectively increase the photocatalytic activity of the ZnS nanoparticles. A possible mechanism to illustrate this was discussed.

(Received September 7, 2015; Accepted October 10, 2015)

Keywords: Carbon nanotubes supported ZnS; Microwave-assisted synthesis;
Photoluminescence properties; Catalytic properties

1. Introduction

Because of their quantum confinement effects and size- and shape-dependent photoemission characteristics, semiconducting metal chalcogenide nanocrystals have been the most intensively studied [1-5]. Many semiconducting nanocrystals of metal sulfides with various compositions and shapes have been synthesized. As an important wide band gap semiconductor, ZnS is widely used in light-emitting diodes[6], photodetectors [7], photochemistry [8], lasers [9], and photoluminescence [10].

Carbon nanotubes (CNTs) are among the most promising nanomaterials because their extraordinary physical, chemical, and mechanical properties [11-13]. CNTs decorated with organic and inorganic compounds through covalent and non-covalent bonds can provide new properties and may lead to new application and thus many CNTs-based nanocomposites were successfully

---

[*] Corresponding author*:* wangguizhen0@hotmail.com

prepared [14-17]. Recently, much works have been focused on the synthesis of decorating CNTs with ZnS nanoparticles to enhance its physical properties and applications. For instance, Gao et al. synthesized CNTs coated with size of less than 4 nm ZnS layers by a simple in-situ synthetic method without causing a significant modification of energy states of the CNTs [18]. Further, CNTs/ZnS core/shell heterostructures prepared by Gu and co-workers using a facile solution-chemical method, which offers the possibility to readily control the thickness of the ZnS shell by adjusting the experimental parameters properly [19]. In addition, Mitra’s group synthesized CNTs/ZnS heterostructures consisting of ZnS nanoparticles of average size 2 nm by a very simple chemical precipitation method without using any capping agent [20]. Nevertheless, it is still very important to develop some other fast methods for the preparation of CNTs supported ZnS nanoparticles with enhanced properties in mild reaction conditions.

For the present research, we successfully prepared CNTs supported ZnS nanoparticles with a dense and homogeneous layer by a simple microwave irradiation method. The as-prepared samples exhibited enhanced photocatalytic activity in the elimination of methylene blue (MB).

2. Experimental

2.1 Preparation

Pristine CNTs made by the chemical vapor deposition method were purchased from Shenzhen Nanoport company (diameter: 20-40 nm, purity>95%). For the better anchoring of the ZnS nanoparticles, CNTs were first oxidized by refluxing in concentrated HNO_3 at 413K for 4 hours [21]. Then purified by distilled water till pH value being neutrality and dried at 333K for 12 hours.

The preparation of CNTs supported ZnS was carried out in glycol (EG) solution. First, 1 mmol $Zn(Ac)_2 \cdot 2H_2O$ and 50 mg of CNTs were added into 20 ml EG in a 50 ml beaker (marked A). The solution A was ultrasonically treated for 1 hours to ensure CNTs being uniformly dispersed in EG solution. Meanwhile, 1 mmol $Na_2S \cdot 9H_2O$ was dissolved in another 20 ml EG (marked B). Then, the solution B was added into the solution A. The new mixture was placed in the center of an improved household microwave oven (Galanz WP750, 2450 MHz, 750 W) with a refluxing system outside. 20% (150 W) of the output power of the microwave was used to irradiate the mixture for 6 min. Then, the microwave heating was terminated and the products were collected by centrifugation, washed with distilled water and absolute ethanol repeatedly for three times, and dried at 45 ºC in vacuum.

2.2 Characterization

X-ray powder diffraction (XRD) analysis was performed on a BRUKER AXS D8 Advance diffractometer with Cu Kα radiation (λ=1.54178 Å) using a 40 kV operation voltage and 40 mA current. The transmission electron microscopy (TEM) images were collected on a JEOL JEM 2100 transmission electron microscope operating at an accelerating voltage of 200 kV. The UV-Vis absorbance spectra were obtained on a UV-Vis spectrophotometer (UV-2450). The photoluminescence (PL) was studied on a Hitachi F-7000 fluorescence spectrophotometer with Xe lamp at room temperature. The resulting products were dispersed in water and measured in a standard quartz cuvette.

2.3 Photocatalytic experiments

A 500 mL glass vessel with a water-cooled quartz jacket was used as a photoreactor vessel. The UV lamp (300 W, main emission was 365 nm) was vertically placed in the center of the quartz jacket. CNTs supported ZnS was added into the reactor containing 450 mL aqueous solution of MB (initial concentration was 26.7 mg/L). After the photocatalysts were added into the aqueous solution under magnetic agitation, the UV illumination was turned on. Air was supplied to the aqueous solution to ensure a constant supply of oxygen and promote a complete mixing of solution and the photocatalyst during photoreaction. All the experiments were carried out at about 25 ^{o}C controlled by the water cooling. 3 mL aliquots were sampled and centrifuged to remove photocatalyst powders for analysis by UV-Vis spectroscopy at given time intervals. The UV-Vis spectrum of the MB solution was recorded on a UV-2450 UV-Vis spectrophotometer. The full spectrum (200-800 nm) of each sample was recorded and the characteristic absorption of MB at 665 nm was chosen as the monitored parameter for the photocatalytic degradation process.

3. Results and discussion

Fig. 1a shows the TEM image of CNTs used in this work after an oxidation treatment in the nitric acid. It can be clearly seen that the CNTs used in this work were well dispersed, and no other foreign particles can be found. The XRD pattern of the CNTs is shown in Fig. 1b. The diffraction peaks at 2θ = 26.0° and 43.8° can be assigned to (002) and (100) planes of graphite phase (JCPDS 75-1621) respectively.

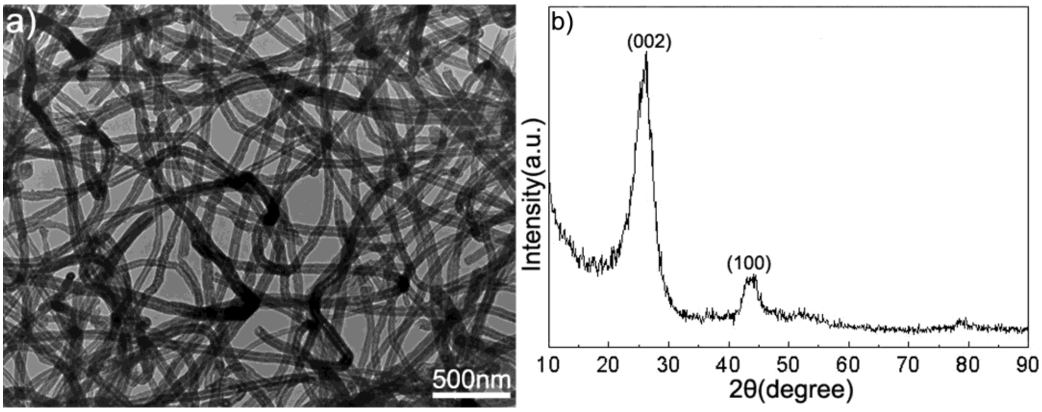

Fig. 1. (a) TEM image and (b) XRD pattern of CNTs

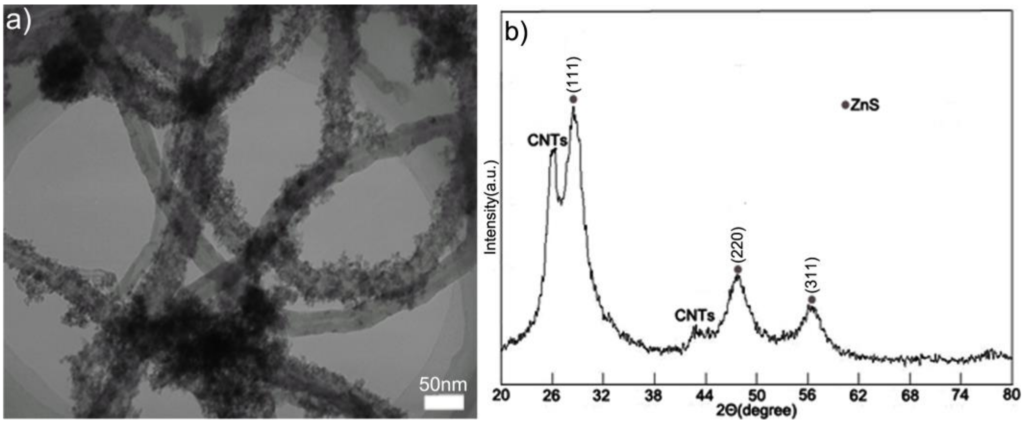

Fig. 2. (a) TEM image and (b) XRD pattern of CNTs supported ZnS nanoparticles

The morphology and microstructure of CNTs supported ZnS nanoparticles are shown in Fig. 2. As TEM image shown in Fig. 2a, the CNTs are decorated with a layer of nanoparticles, and no free nanoparticles are found. The size of the Ni particles estimated from the TEM Fig. 2a observation is about 1.0-1.5 nm. Moreover, the particles were firmly fixed on the CNTs as the nanoparticles could not be removed by thorough washing, severe agitation and ultrasonic processing. Fig. 2b shows the XRD pattern of CNTs supported ZnS nanoparticles. Except CNTs, the other three diffraction peaks could be indexed as the sphalerite crystal ZnS (JCPDS 65-1691, a = 0.5410 nm). The average size of ZnS crystallite calculated from the width of the reflection according to the Debye-Scherrer equation was about 1.1 nm.

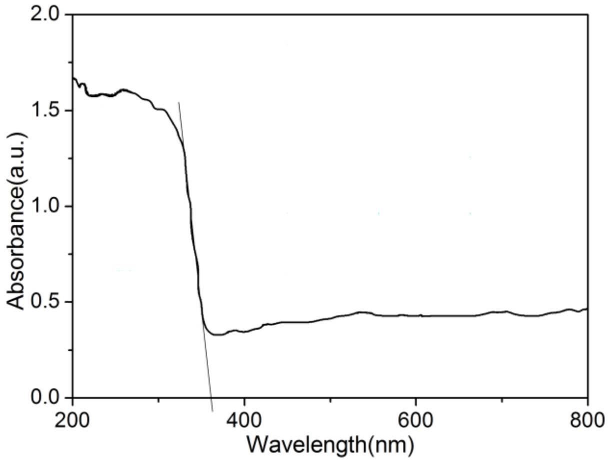

Fig. 3. UV-Vis absorbance spectrum of CNTs supported ZnS nanoparticles

Fig. 3 shows the UV-Vis absorbance spectra of CNTs supported ZnS nanoparticles. It is clear that CNTs supported ZnS nanoparticles have fundamental absorption shape edge rising at about 370 nm, similar to pure ZnS nanoparticles, and also has absorption flat in the region of visible light derived from CNTs.

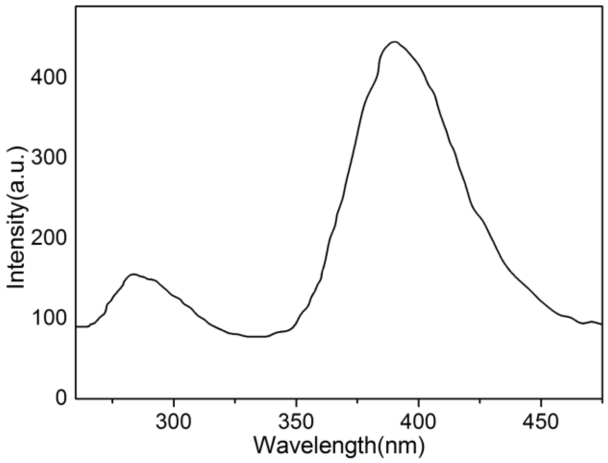

Fig. 4. PL spectrum recorded at room temperature of CNTs supported ZnS nanoparticles

The room-temperature PL spectrum of CNTs supported ZnS nanoparticles are shown in Fig. 4, which were measured from 250 to 475 nm using a 245 nm exciting wavelength. Two emission bands have been observed in the PL spectrum of CNTs supported ZnS nanoparticles. One is at 391 nm while the other is at about 283 nm. The peak at 391 nm is attributed to the trap states emission of ZnS nanocrystals due to the broad feature. The peak at 283 nm has been assigned to the band edge emission. The absorption edges are shifted to higher energies from the bulk band gap of ZnS. We considered that the blue shift of the emission components could be related to the quantum-sized effect from ZnS nanoparticles.

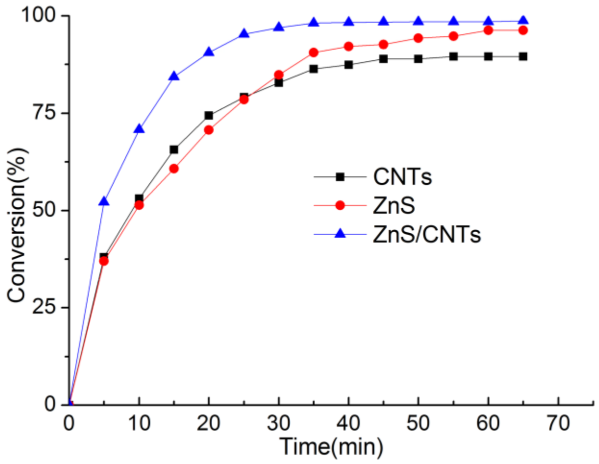

Fig. 5. Photodegradation of MB with CNTs, ZnS, and CNTs supported ZnS photocatalysts

In order to evaluate the photocatalytic activities of as-synthesized CNTs supported ZnS nanoparticles, the degradation ability of MB in water under 300 W UV lamp irradiation was studied. As shown in Fig. 5, it is more interesting that we have found the complete decomposition of MB (more than 96% of the initial concentration) under UV exposure in the presence of ZnS nanoparticles was obtained after about 65 min, and that in presence of CNTs supported ZnS nanoparticles was obtained only after about 35 min. This result demonstrates that CNTs can effectively enhance the photocatalytic activity of ZnS nanoparticles. This reason may be related to the strong interfacial connection between ZnS nanoparticles and CNTs, which promotes interfacial electron transfer from the attached ZnS to the nanotubes and then retards the recombination of the e^-/h^+ pairs of ZnS nanoparticles. Additionally, CNTs as catalyst support can prevent ZnS nanoparticles from aggregating, which may be another factor for enhancing the photocatalytic efficiency of ZnS nanoparticles.

4. Conclusions

In this work, CNTs coated with ZnS nanoparticles were fabricated by a simple microwave irradiation method. A dense and homogeneous layer of ZnS nanoparticles with the diameter of about 1.1 nm can be obtained on the surface of CNTs. The PL spectrum shows that the PL peaks of the CNTs supported ZnS have a small blue shift in comparison with the bulk of ZnS. Moreover, CNTs can effectively promote the photocatalvtic activity of ZnS nanoparticles in the elimination of MB. This result may be related to the strong interfacial connection between ZnS nanoparticles and CNTs, which promotes interfacial electron transfer from the attached ZnS to CNTs and then retards the recombination of the e^-/h^+ pairs of ZnS nanoparticles. CNTs as catalyst support can prevent ZnS nanoparticles from aggregating, which may be another factor for enhancing the photocatalytic efficiency of ZnS nanoparticles. The method presented here may be extended to synthesize other composites based on coating CNTs with semiconductor nanoparticles via the microwave irradiation method.

Acknowledgements

This work was supported by the National Natural Science Foundation of China (11564011, 51362010), the Natural Science Foundation of Hainan Province (514207, 514212), the Scientific Research Projects of Colleges and Universities of Hainan Province (HNKY2014-14), and the Scientific Research Projects of Hainan University (kyqd1502).

References

[1] Y. Zhao, Y. Zhang, H. Zhu, G. C. Hadjipanayis, J. Q. Xiao, Journal of the American Chemical Society, **126**, 6874(2004).
[2] D. K. Dwivedi, V. Kumar, M. Dubey, H. P. Pathak, Chalcogenide Letters, **8**, 521(2011).
[3] Y. Ma, L. Qi, J. Ma, H. Cheng, W. Shen, Langmuir, **19**, 9079(2003).
[4] S. M. Lee, Y. Jun, S. N. Cho, J. Cheon, Journal of the American Chemical Society, **124**, 11244(2002).
[5] B. Denac, M. Kristl, M. Drofenik, Chalcogenide Letters, **8**, 427(2011).
[6] W. Tang, D. C. Cameron, Thin Solid Films, **280**, 221(1996).
[7] E. Monroy, F. Omnes, F. Calle, Semiconductor science and technology, **18**, R33(2003).
[8] Y. Wada, T. Kitamura, S. Yanagida, H. Yin, Chemmical Communications, **24**, 2683(1998).
[9] C. Falcony, M. Garcia, A. Ortiz, J. Alonso, Journal of applied physics, **72**, 1525(1992).
[10] H. Wang, H. Li, Chalcogenide Letters, **8**, 249(2011).

[11] A. Star, E. Tu, J. Niemann, J. C. P. Gabriel, C. S. Joiner, C. Valcke, Proceedings of the National Academy of Sciences of the United States of America, **103**, 921(2006).
[12] Z. Liu, W. Cai, L. He, N. Nakayama, K. Chen, X. Sun, X. Chen, H. Dai, Nature Nanotechnology, **2**, 47(2007).
[13] K. Kostarelos, L. Lacerda, G. Pastorin, W. Wu, S. Wieckowski, J. Luangsivilay, S. Godefroy, D. Pantarotto, J. P. Briand, S. Muller, Nature Nanotechnology, **2**, 108(2007).
[14] W. Q. Han, A. Zettl, Nano Letters, **3**, 681(2003).
[15] C. Li, Y. Tang, K. Yao, F. Zhou, Q. Ma, H. Lin, M. Tao, J. Liang, Carbon, **44**, 2021(2006).
[16] Y. Liu, J. Tang, X. Chen, W. Chen, Carbon, **44**, 381(2006).
[17] Y. Zhu, H. I. Elim, Y. L. Foo, T. Yu, Y. Liu, W. Ji, J. Y. Lee, Z. Shen, A. T. S. Wee, J. T. L. Thong, Advanced Materials, **18**, 587(2006).
[18] L. Zhao, L. Gao, Journal of Materials Chemistry, **14**, 1001(2004).
[19] F. Gu, C. Li, S. Wang, Inorganic Chemistry, **46**, 5343(2007).
[20] R. Paul, P. Kumbhakar, A. Mitra, Journal of Experimental Nanoscience, **5**, 363(2010).
[21] T. W. Ebbesen, H. Hiura, M. E. Bisher, M. M. J. Treacy, J. L. Shreeve ‑ Keyer, R. C. Haushalter, Advanced Materials, **8**, 155(1996).